To cite this article: Hu J Z, Tang G Y, Wang J J, et al. Swarm control of USVs based on adaptive backstepping combined with sliding mode [J/OL]. Chinese Journal of Ship Research, 2019, 14(6). http://www. ship-research.com/EN / Y2019/V14/I6/1.

DOI:10.19693/j.issn.1673-3185. 01521

Swarm control of USVs based on adaptive backstepping combined with sliding mode

Hu Jianzhang, Tang Guoyuan, Wang Jianjun, Xie De*

School of Naval Architecture and Ocean Engineering, Huazhong University of Science and Technology, Wuhan 430074, China

Abstract: [**Objectives**] In view of the problem about the control of the swarm system composed of several underactuated Unmanned Surface Vehicles (USVs), the control strategy of virtual structure method is studied. [**Methods**] In this paper, the problem about the swarm control was transformed into a problem about the stabilization of the pose tracking error between the USVs and the virtual structure. The formation transformation of USV swarm was realized based on the changed geometry of the virtual structure. The design of the swarm controller was divided into two parts, i.e. kinematics and dynamics. With adequate consideration of the uncertainty disturbance, the underactuated USV swarm controller was proposed based on adaptive backstepping techniques combined with the sliding-mode control method. The stability of the closed loop system was demonstrated by the Lyapunov theory. The simulation test of straight and curve course running and swarm formation transformation were carried out. [**Results**] The simulation results show that the synergy of the USV swarm is remarkable, the formation transformation is smooth, and the UAV swarm can adapt to various uncertain disturbances. [**Conclusions**] The swarm system shows strong robustness and flexibility which lays a theoretical foundation for subsequent USV swarm tests.

Key words: swarm control; underactuated USV; virtual structure; self-adaption; backstepping; sliding-mode control

CLC number: U661.3

0 Introduction

Coordinated and orderly large-scale group behaviors are very common in nature, such as ant colonies, fish swarms, bird flocks, etc. Although individuals in these groups have simple behaviors and limited capabilities, they can complete very complicated tasks when they work together. Humans have created the concept of unmanned swarm by imitating group behavior in nature. Unmanned Surface Vehicles (USVs) swarm, as an unmanned marine intelligent carrier platform, have extremely wide applications in the military and civilian fields including anti-submarine, anti-torpedo, intelligence surveillance and reconnaissance, as well as marine environment monitoring, and marine weather forecasting [1-3]. Moreover, the USV and its swarm have the advantage of operating between sea-air interfaces, which can be used as a communication relay station between the underwater autonomous submersible vehicle and the aerial

Received: 2019 - 01 - 23

Supported by: Fundamental Research Funds for the Central Universities (2018KFYYXJJ012, 2018JYCXJJ045); Foundation of Marine Defense Technology Innovation Center

Authors: Hu Jianzhang, male, born in 1994, master degree candidate. Research interest: motion control of ships and underwater vehicles. E-mail: hujzz@qq.com

Tang Guoyuan, male, born in 1973, Ph.D., associate professor. Research interest: motion control of ships and underwater vehicles, marine electromechanical control system and special equipment system, marine power plant. E-mail: tgyuan@hust.edu.cn

Wang Jianjun, male, born in 1987, Ph.D., lecturer. Research interest: deep sea mechanical and electrical equipment technology. E-mail: wangjianjun@hust.edu.cn

Xie De, male, born in 1964, Ph.D., professor. Research interest: design and manufacture of ships and marine structures. E-mail: dexie@hust.edu.cn

***Corresponding author:** Tang Guoyuan

drone, so as to act as the key node of the three-dimensional ocean space.

In recent years, the control of USVs has become a research hotspot in the field of control, which has aroused the attention of many scholars. At the same time, a large number of research results have also obtained [4-8]. According to different control strategies, several methods can be adopted including the leader-follower method, behavior-based method, artificial potential field method, and virtual structure method. Using the leader-follower method, Ding et al. [9] established the mathematical model of USV swarm and designed a backstepping controller to enable USV swarm to sail in the expected formation. Using an artificial potential field method and considering USV swarm avoidance and formation realization simultaneously, Song et al. [10] studied the swarm formation control based on the potential function and Multi-agent theory. Monteiro et al. [11] adopted the behavior-based swarm control method to solve the real-time obstacle avoidance problem of nonlinear systems and obtained the ideal swarm motion trajectory. Zhao et al. [12] combined the virtual structure method and artificial potential field method and then introduced a potential collision function to the relative collision function, which realized cooperative collision avoidance and obstacle avoidance of USV swarm. In the above methods, the leader-follower method relies heavily on the state of the leader, and the swarm system is not robust enough. The behavior-based method is hard to use precise mathematical methods to analyze and ensure the stability of the swarm. The artificial potential field method has the problem of the local optimal solution; hence, it is difficult to construct an appropriate potential function.

In this paper, based on the control strategy of the virtual structure method, a dynamic model of pose tracking error between each USV and the corresponding point of the virtual structure is established, and the swarm control is simplified to the stabilization control of the tracking error. By adding the geometric parameter of the virtual structure to the controller, the formation of the UAVs is changed to increase the flexibility of the system. The controller design is divided into two parts: kinematics and dynamics. Considering factors including the system's own uncertainty and external environmental disturbance, based on Lyapunov stability theory, an adaptive disturbance observer is designed to make compensation in the controller so as to achieve adaptive backstepping sliding-mode control of underactuated USVs.

1 Description of control problem

1.1 Mathematical model of USVs

For the motion control problems of most USVs (such as heading control and trajectory control), the three-degree-of-freedom motion of the horizontal plane is mainly considered. The non-linear mathematical model of the horizontal motion for a single underactuated USV can be expressed as [10]

$$\begin{cases} \dot{\boldsymbol{\eta}} = \boldsymbol{R}(\psi)\boldsymbol{v} \\ \boldsymbol{M}\dot{\boldsymbol{v}} = -\boldsymbol{C}(\boldsymbol{v})\boldsymbol{v} - \boldsymbol{D}(\boldsymbol{v})\boldsymbol{v} + \boldsymbol{\tau} + \boldsymbol{\tau}_{\mathrm{E}} \end{cases} \tag{1}$$

where $\boldsymbol{\eta} = \begin{bmatrix} x & y & \psi \end{bmatrix}^{\mathrm{T}}$ and $\boldsymbol{v} = \begin{bmatrix} u & v & r \end{bmatrix}^{\mathrm{T}}$ are three degrees of freedom of USVs moving on the horizontal plane and their velocity vectors; $\boldsymbol{R}(\psi) = \begin{bmatrix} \cos\psi & -\sin\psi & 0 \\ \sin\psi & \cos\psi & 0 \\ 0 & 0 & 1 \end{bmatrix}$ is the rotation matrix; $\boldsymbol{C}(v) = \begin{bmatrix} 0 & 0 & -m_{22}v \\ 0 & 0 & m_{11}u \\ m_{22}v & -m_{11}u & 0 \end{bmatrix}$ refers to Coriolis force and centripetal force matrices; $\boldsymbol{M} = \mathrm{diag}(m_{11}, m_{22}, m_{33})$ denotes inertial matrix; $\boldsymbol{D}(v) = \mathrm{diag}(d_{11}, d_{22}, d_{33})$ means hydrodynamic damping matrix; $\boldsymbol{\tau} = \begin{bmatrix} \tau_u & 0 & \tau_r \end{bmatrix}^{\mathrm{T}}$ indicates propulsion and steering torque vectors of USVs; $\boldsymbol{\tau}_{\mathrm{E}} = \begin{bmatrix} \tau_{\mathrm{E}u} & \tau_{\mathrm{E}v} & \tau_{\mathrm{E}r} \end{bmatrix}^{\mathrm{T}}$ is the uncertain disturbance including the uncertainty of the system itself, and external environmental disturbance.

1.2 Control strategy

This paper adopts a swarm control strategy based on the virtual structure method to achieve USVs control, and its flow chart of control strategy is shown in Fig. 1. According to the task of the swarm operation, this paper designs the virtual structure and defines its movement behavior. The fixed reference points in the virtual structure of each USV are controlled so as to maintain the formation of the swarm. By transforming the geometry of the virtual structure, we transform the corresponding swarm formation to meet the needs of various swarm tasks.

Fig. 2 shows the formation structure and tracking errors of USVs. In the figure, $O-xy$ is the geodetic coordinate system and $o-uv$ is the satellite coordinate system. A virtual rigid body structure is designed, and an arbitrary point in the structure is selected as the reference point, which is expected to move according to the desired trajectory $\Omega(x_{\mathrm{d}}, y_{\mathrm{d}})$. The pose of other points in the structure can be expressed by the distance l and the angle θ from the

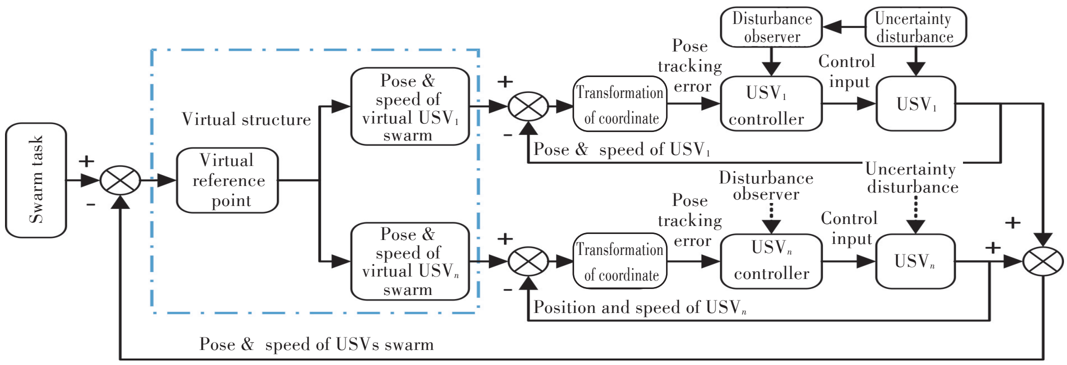

Fig.1 Flow chart of control strategy for USVs

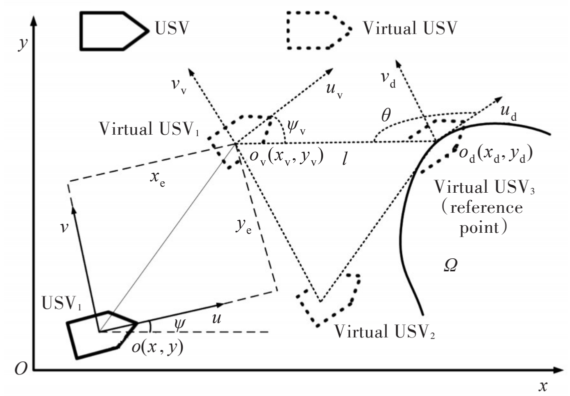

Fig.2 Formation structure and tracking errors of USVs

reference point:

$$\boldsymbol{\eta}_{\mathrm{v}}=\boldsymbol{\eta}_{\mathrm{d}}+\boldsymbol{R}(\psi_{\mathrm{d}})\boldsymbol{l} \tag{2}$$

where $\boldsymbol{\eta}_{\mathrm{v}}=\begin{bmatrix}x_{\mathrm{v}} & y_{\mathrm{v}} & \psi_{\mathrm{v}}\end{bmatrix}^{\mathrm{T}}$ is the pose of any point in the virtual structure; $\boldsymbol{\eta}_{\mathrm{d}}=\begin{bmatrix}x_{\mathrm{d}} & y_{\mathrm{d}} & \psi_{\mathrm{d}}\end{bmatrix}^{\mathrm{T}}$ denotes the pose of reference point; $\boldsymbol{R}(\psi_{\mathrm{d}})$ refers to rotation matrix; $\boldsymbol{l}=\begin{bmatrix}l_x & l_y & 0\end{bmatrix}^{\mathrm{T}}=\begin{bmatrix}l\cos\theta & l\sin\theta & 0\end{bmatrix}^{\mathrm{T}}$.

Each point in the virtual structure is considered as a virtual USV with similar dynamic characteristics to each USV, and its mathematical model can be established according to Eq. (1). Because virtual USV has no driving force or moment, its mathematical model can be expressed as

$$\begin{cases}\dot{\boldsymbol{\eta}}_{\mathrm{v}}=\boldsymbol{R}(\psi_{\mathrm{v}})\boldsymbol{v}_{\mathrm{v}}\\ \dot{v}_{\mathrm{v}}=\dfrac{1}{m_{22}}(m_{11}u_{\mathrm{v}}r_{\mathrm{v}}-d_{22}v_{\mathrm{v}}+\tau_{\mathrm{E}v})\end{cases} \tag{3}$$

where $\boldsymbol{R}(\psi_{\mathrm{v}})$ refers to the rotation matrix; $\boldsymbol{v}_{\mathrm{v}}=\begin{bmatrix}u_{\mathrm{v}} & v_{\mathrm{v}} & r_{\mathrm{v}}\end{bmatrix}^{\mathrm{T}}=\begin{bmatrix}u_{\mathrm{d}}-l_y r_{\mathrm{d}} & v_{\mathrm{d}}+l_x r_{\mathrm{d}} & r_{\mathrm{d}}\end{bmatrix}^{\mathrm{T}}$ means the speed of virtual USV, and $u_{\mathrm{d}}, v_{\mathrm{d}}, r_{\mathrm{d}}$ are the speeds of reference point.

In order to facilitate the design of the controller, the pose tracking error between the USV and the virtual USV is transformed from the coordinate system $O-xy$ to the coordinate system $o-uv$:

$$\begin{bmatrix}x_{\mathrm{e}}\\ y_{\mathrm{e}}\\ \psi_{\mathrm{e}}\end{bmatrix}=\boldsymbol{R}^{\mathrm{T}}(\psi)\begin{bmatrix}x-x_{\mathrm{v}}\\ y-y_{\mathrm{v}}\\ \psi-\psi_{\mathrm{v}}\end{bmatrix} \tag{4}$$

Differentiating both sides of Eq. (4) and combining Eq. (1) and Eq. (3), we can obtain the pose tracking error model:

$$\begin{cases}\dot{x}_{\mathrm{e}}=u-u_{\mathrm{v}}\cos\psi_{\mathrm{e}}-v_{\mathrm{v}}\sin\psi_{\mathrm{e}}+ry_{\mathrm{e}}\\ \dot{y}_{\mathrm{e}}=v_{\mathrm{e}}+u_{\mathrm{v}}\sin\psi_{\mathrm{e}}-v_{\mathrm{v}}(\cos\psi_{\mathrm{e}}-1)-rx_{\mathrm{e}}\\ \dot{\psi}_{\mathrm{e}}=r-r_{\mathrm{v}}\\ \dot{u}=\dfrac{1}{m_{11}}(m_{22}vr-d_{11}u+\tau_u+\tau_{\mathrm{E}u})\\ \dot{v}_{\mathrm{e}}=-\alpha(ur-u_{\mathrm{v}}r_{\mathrm{v}})-\beta v_{\mathrm{e}}\\ \dot{r}=\dfrac{1}{m_{33}}((m_{11}-m_{22})uv-d_{33}r+\tau_r+\tau_{\mathrm{E}r})\end{cases} \tag{5}$$

where $v_{\mathrm{e}}=v-v_{\mathrm{v}}$; $\alpha=m_{11}/m_{22}$; $\beta=d_{22}/m_{22}$.

Therefore, the issue of underactuated USVs control in this paper is simplified to the stabilization control of Eq. (5).

1.3 Control objectives

Control objectives: For the control of a swarm system composed of multiple underactuated USVs, the control strategy of the virtual structure method is adopted, and the control rates τ_u and τ_r are designed to stabilize the pose tracking error of the swarm system to a sufficiently small range near the origin point, so as to achieve the swarm operation of USVs.

According to the control objectives, the following hypotheses are made before designing the controller:

Hypothesis 1: The uncertainty term τ_{E} is bounded, but its upper bound is unknown, namely $|\tau_{\mathrm{E}}|\leqslant\tau_{\mathrm{E\,max}}<\infty$ 。

Hypothesis 2: Only the situation that each USV is sailing forward without reversing is considered, namely $u>0$ and $u>|v|$.

2 Controller design

2.1 Kinematics of controller design

First, this paper designs the kinematics loop and considers the surge velocity u as the input of the subsystem x_{e}. According to the expression of $\dot{x}_{\mathrm{e}}$, u^{α} is designed as

$$u^{\alpha}=-k_1x_{\mathrm{e}}+u_{\mathrm{v}} \tag{6}$$

where u^{α} is the virtual control amount of u and k_1 is a positive constant.

In order to simplify the problem, the coordinate transformation $z_{\mathrm{e}}=y_{\mathrm{e}}+v_{\mathrm{e}}/\beta$ is introduced to eliminate the term v_{e}. Substituting Eq. (6) after the derivation of z_{e}, we can obtain

$$\dot{z}_{\mathrm{e}}=u_{\mathrm{v}}\sin\psi_{\mathrm{e}}-v_{\mathrm{v}}(\cos\psi_{\mathrm{e}}-1)-rx_{\mathrm{e}}-\frac{\alpha}{\beta}\left((-k_1x_{\mathrm{e}}+u_{\mathrm{v}})r-u_{\mathrm{v}}r_{\mathrm{v}}\right)-\frac{\alpha}{\beta}u_{\mathrm{e}}r \tag{7}$$

Taking $k_1=\beta/\alpha$ to eliminate the term x_{e}, we can reduce Eq. (7) to

$$\dot{z}_{\mathrm{e}}=u_{\mathrm{v}}\sin\psi_{\mathrm{e}}-v_{\mathrm{v}}(\cos\psi_{\mathrm{e}}-1)-\frac{\alpha u_{\mathrm{v}}}{\beta}(r-r_{\mathrm{v}})-\frac{\alpha}{\beta}u_{\mathrm{e}}r \tag{8}$$

Taking the heading angle deviation ψ_{e} as the input of subsystem z_{e}, according to the expression of $\dot{z}_{\mathrm{e}}$, we can design $\psi_{\mathrm{e}}^{\alpha}$ as

$$\psi_{\mathrm{e}}^{\alpha}=-\arcsin\left(\frac{k_2z_{\mathrm{e}}}{\Delta}\right) \tag{9}$$

where $\psi_{\mathrm{e}}^{\alpha}$ is the virtual control amount of ψ_{e} and k_2 is a positive constant, $\Delta=\sqrt{1+(k_2z_{\mathrm{e}})^2}$.

Defining the error amount of the heading angle deviation as $w_{\mathrm{e}}=\psi_{\mathrm{e}}-\psi_{\mathrm{e}}^{\alpha}$, and taking the derivative of w_{e}, there is we can obtain

$$\dot{w}_{\mathrm{e}}=\left(1-k_2\alpha u_{\mathrm{v}}/(\beta\Delta^2)\right)(r-r_{\mathrm{v}})+\frac{k_2}{\Delta^2}\left(u_{\mathrm{v}}\sin\psi_{\mathrm{e}}-v_{\mathrm{v}}(\cos\psi_{\mathrm{e}}-1)\right)-\frac{k_2\alpha u_{\mathrm{e}}r}{\beta\Delta^2} \tag{10}$$

Considering the yawing angular velocity r as the input of the subsystem w_{e}, r^{α} can be expressed as

$$r^{\alpha}=\frac{1}{1-k_2\alpha u_{\mathrm{v}}/(\beta\Delta^2)}\cdot\left(-k_3w_{\mathrm{e}}-\frac{k_2}{\Delta^2}\left(u_{\mathrm{v}}\sin\psi_{\mathrm{e}}-v_{\mathrm{v}}(\cos\psi_{\mathrm{e}}-1)\right)\right)+r_{\mathrm{v}} \tag{11}$$

where r^{α} is the virtual control amount of r and k_3 is a positive constant.

2.2 Dynamics of controller design

Defining the surge velocity error $u_{\mathrm{e}}=u-u^{\alpha}$ and selecting the sliding mode surface $s_u=u_{\mathrm{e}}$, the derivation of s_u can be expressed as

$$\dot{s}_u=\dot{u}_{\mathrm{e}}=\frac{1}{m_{11}}(m_{22}vr-d_{11}u+\tau_u+\tau_{\mathrm{E}u})-\dot{u}^{\alpha} \tag{12}$$

The exponential approach law is utilized $\dot{s}=-\lambda\,\mathrm{sgn}\,s-ks\ (\lambda>0,\,k>0)$:

$$\tau_u=-\lambda_1m_{11}\,\mathrm{sgn}(s_u)-k_4m_{11}s_u-m_{22}vr+d_{11}u+m_{11}\dot{u}^{\alpha} \tag{13}$$

where λ_1 and k_4 are positive constants.

Similarly, the error quantity of yawing angular velocity is defined as $r_{\mathrm{e}}=r-r^{\alpha}$, and the sliding mode surface $s_r=r_{\mathrm{e}}$ is selected and derived as

$$\dot{s}_r=\dot{r}_{\mathrm{e}}=\frac{1}{m_{33}}((m_{11}-m_{22})uv-d_{33}r+\tau_r+\tau_{\mathrm{E}r})-\dot{r}^{\alpha} \tag{14}$$

The exponential approach law is also adopted

$$\tau_r=-\lambda_2m_{33}\,\mathrm{sgn}(s_r)-k_5m_{33}s_r-(m_{11}-m_{22})uv+d_{33}r+m_{33}\dot{r}^{\alpha} \tag{15}$$

where λ_2 and k_5 are positive constants.

For uncertain interference, an adaptive interference observer is designed

$$\begin{cases}\dot{\zeta}_u=k_4s_u+\lambda_1\,\mathrm{sgn}(s_u)\\ \hat{\tau}_{\mathrm{E}u}=k_6m_{11}(\zeta_u+s_u)\end{cases} \tag{16}$$

$$\begin{cases}\dot{\zeta}_r=k_6s_r+\lambda_2\,\mathrm{sgn}(s_r)\\ \hat{\tau}_{\mathrm{E}u}=k_7m_{33}(\zeta_r+s_r)\end{cases} \tag{17}$$

where ζ_u and ζ_r are auxiliary control terms; $\hat{\tau}_{\mathrm{E}u}$ and $\hat{\tau}_{\mathrm{E}r}$ are respectively the estimated values of τ_{Eu} and $\tau_{\mathrm{E}r}$; k_6 and k_7 are positive constants.

Then, Eq. (13) and Eq. (15) can be rewritten as

$$\tau_u=-\lambda_1m_{11}\,\mathrm{sgn}(s_u)-k_4m_{11}s_u-m_{22}vr+d_{11}u+m_{11}\dot{u}^{\alpha}-\hat{\tau}_{\mathrm{E}u} \tag{18}$$

$$\tau_r=-\lambda_2m_{33}\,\mathrm{sgn}(s_r)-k_5m_{33}s_r-(m_{11}-m_{22})uv+d_{33}r+m_{33}\dot{r}^{\alpha}-\hat{\tau}_{\mathrm{E}r} \tag{19}$$

So far, the design of underactuated USVs controllers based on the adaptive backstepping combined with sliding mode has been completed, i.e., Eq. (18)–Eq. (19).

3 Stability analysis

Theorem 1: For the control problem of a swarm system composed of multiple underactuated USVs, under the conditions of Hypothesis 1 and Hypothesis 2, this paper designs an adaptive backstepping sliding–mode controller, as shown in Eq. (18)–Eq. (19). Appropriate control parameters $k_i(1\leqslant i\leqslant 7)$ and $\lambda_j(1\leqslant j\leqslant 2)$ make the pose tracking error of the swarm system gradually converge to a small enough neighborhood near the origin point, namely that, the error is consistent and ultimately bounded, so as to achieve the swarm control goal of USVs.

The equation demonstration is as follows.

According to the control quantity designed in the previous section, the error system can be rearranged:

$$\begin{cases}\dot{x}_{\rm e}=-k_1x_{\rm e}+u_{\rm e}-u_{\rm v}\left(\cos\left(\psi_{\rm e}^{\alpha}+w_{\rm e}\right)-1\right)-v_{\rm v}\sin\left(\psi_{\rm e}^{\alpha}+w_{\rm e}\right)+\left(r^{\alpha}+r_{\rm e}\right)\left(z_{\rm e}-v_{\rm e}/\beta\right)\\ \dot{z}_{\rm e}=\dfrac{-k_2u_{\rm v}z_{\rm e}}{\Delta}+u_{\rm v}\left(\sin\psi_{\rm e}^{\alpha}\left(\cos w_{\rm e}-1\right)+\cos\psi_{\rm e}^{\alpha}\sin w_{\rm e}\right)-v_{\rm v}\left(\cos\left(\psi_{\rm e}^{\alpha}+w_{\rm e}\right)-1\right)-\dfrac{\alpha u_{\rm v}}{\beta}\left(r^{\alpha}+r_{\rm e}-r_{\rm v}\right)-\dfrac{\alpha}{\beta}u_{\rm e}r\\ \dot{w}_{\rm e}=-k_3w_{\rm e}+\left(1-k_2\alpha u_{\rm v}\big/\left(\beta\Delta^2\right)\right)r_{\rm e}-\dfrac{k_2\alpha u_{\rm e}r}{\beta\Delta^2}\\ \dot{u}_{\rm e}=-k_4u_{\rm e}-\lambda_1\operatorname{sgn}\left(u_{\rm e}\right)+\dfrac{\tilde{\tau}_{{\rm E}u}}{m_{11}}\\ \dot{v}_{\rm e}=-\alpha\left(\left(u^{\alpha}+u_{\rm e}\right)\left(r^{\alpha}+r_{\rm e}\right)-u_{\rm v}r_{\rm v}\right)-\beta v_{\rm e}\\ \dot{r}_{\rm e}=-k_5r_{\rm e}-\lambda_2\operatorname{sgn}\left(r_{\rm e}\right)+\dfrac{\tilde{\tau}_{{\rm E}r}}{m_{33}}\\ \dot{\tilde{\tau}}_{{\rm E}u}=\dot{\tau}_{{\rm E}u}-k_6\left(\tau_{{\rm E}u}-\hat{\tau}_{{\rm E}u}\right)\\ \dot{\tilde{\tau}}_{{\rm E}r}=\dot{\tau}_{{\rm E}r}-k_7\left(\tau_{{\rm E}r}-\hat{\tau}_{{\rm E}r}\right)\end{cases} \tag{20}$$

where $\tilde{\tau}_{{\rm E}u}=\tau_{{\rm E}u}-\hat{\tau}_{{\rm E}u}$, $\tilde{\tau}_{Er}=\tau_{{\rm E}r}-\hat{\tau}_{{\rm E}r}$ are errors of the interference observer.

The Lyapunov function is defined as $V=\frac{1}{2}(\tilde{\tau}^2_{{\rm E}u}+\tilde{\tau}^2_{{\rm E}r}+u_{\rm e}^2+r_{\rm e}^2+w_{\rm e}^2+z_{\rm e}^2+x_{\rm e}^2+\frac{v_e^2}{\beta^2})$ is defined and its derivation is

$$\dot{V}\leqslant-k_1x_{\rm e}^2-k_3w_{\rm e}^2-k_4u_{\rm e}^2-k_5r_{\rm e}^2-k_6\tilde{\tau}^2_{{\rm E}u}-k_7\tilde{\tau}^2_{{\rm E}r}-\lambda_1\left|u_{\rm e}\right|-\lambda_2\left|r_{\rm e}\right|-\frac{1}{\beta}v_{\rm e}^2-k_2\left(1+\frac{k_2\alpha u_{\rm v}}{\beta-k_2\alpha u_{\rm v}}\right)\cdot\frac{\left(u_{\rm v}-\left|v_{\rm v}\right|\right)z_{\rm e}^2}{\Delta}+\dot{\tau}_{{\rm E}u}\tilde{\tau}_{{\rm E}u}+\dot{\tau}_{{\rm E}r}\tilde{\tau}_{{\rm E}r} \tag{21}$$

According to Hypothesis 2, $u_{\rm v}>0$ and $u_{\rm v}>\left|v_{\rm v}\right|$. To satisfy $\frac{k_2\alpha u_{\rm v}}{\beta-k_2\alpha u_{\rm v}}+1>0$, we should set $0<k_2<\beta/\alpha u_{\rm v}$. According to Hypothesis 1, since $\tau_{\rm E}$ is bounded, the error system Eq. (20) can be guaranteed to be uniformly bounded. By adjusting the parameters, the final boundary value is guaranteed to be small enough, which means that theorem 1 is proved.

4 Simulation test

This paper assumes that the control laws Eq. (18)–Eq. (19) based on adaptive backstepping in combination with sliding mode are the control law 1, and the general backstepping sliding-mode control laws Eq. (13) and Eq. (15) are the control law 2. For the swarms with three identical underactuated USVs, control laws 1 and 2 are adopted for simulation tests. In addition, test results are compared to verify the correctness and effectiveness of the control method in this paper.

The total length of the USV is 4.68 m, with the width of 1.70 m, the depth of 0.55 m, the draft of 0.40 m, and the hull mass of 538 kg. The model parameters of the USV are m_{11} = 646 kg, m_{22} = 837 kg, m_{33} = 155 kg · m^2, d_{11} = 303 kg/s, d_{22} = 425 kg/s, d_{33} = 74 (kg · m^2)/s. Assuming that the modeling error is 10% and considering the extreme conditions in the simulation test, the model parameters of the USV are set as 1.1m_{11}, 0.9m_{22}, 0.9m_{33}, 0.9d_{11}, 1.1d_{22}, 1.1d_{33}.

Assuming that the time-varying external disturbance is

$$\begin{cases}\tau_{{\rm E}u}=0.2\cdot m_{11}\left(\sin\left(0.05t\right)+1\right)\\ \tau_{{\rm E}v}=0.1\cdot m_{22}\left(\sin\left(0.04t\right)+0\right)\\ \tau_{{\rm E}u}=0.5\cdot m_{33}\left(\sin\left(0.05t+\pi/4\right)+2\right)\end{cases}$$

The initial state of the three USVs in the given swarm is

$$\left[x_1(0)\quad y_1(0)\quad \psi_1(0)\quad u_1(0)\quad v_1(0)\quad r_1(0)\right]=\left[-5\quad 2\quad -\pi/12\quad 0\quad 0\quad 0\right]$$

$$\left[x_2(0)\quad y_2(0)\quad \psi_2(0)\quad u_2(0)\quad v_2(0)\quad r_2(0)\right]=\left[-5\quad 5\quad \pi/12\quad 0\quad 0\quad 0\right]$$

$$\left[x_3(0)\quad y_3(0)\quad \psi_3(0)\quad u_3(0)\quad v_3(0)\quad r_3(0)\right]=\left[-5\quad 0\quad -\pi/6\quad 0\quad 0\quad 0\right]$$

Controller parameters are chosen as follows: $k_1=\beta/\alpha=0.66$, $k_2=0.10$, $k_3=k_4=k_5=k_6=k_7=1.10$, $\lambda_1=\lambda_2=0.20$, where $\alpha=m_{11}/m_{22}=0.94$, and $\beta=d_{22}/m_{22}=0.62$.

The specific process of the simulation test is as follows:

1) In the initial 50 s, the expected formation of the USV swarm is set to the in-line form, namely $l_1=0$, $\theta_1=0$, $l_2=20$, $\theta_2=\pi/2$, $l_3=20$, $\theta_3=-\pi/2$, and the expected trajectory is a straight line coinciding with the x-axis, with the expected sailing speed of $u_{\rm d}=2$ m/s.

2) For the next 50 s, the trajectory is kept unchanged, and the expected speed of the swarm is reduced to $u_{\rm d}=1$ m/s, with the formation changing to a triangle form, namely $l_1=0$, $\theta_1=0$, $l_2=10$,

$\theta_2=2\pi/3, l_3=10$, $\theta_3=-2\pi/3$.

3) For the final 300 s, with the unchanged formation and speed, the USV swarm will follow the S-shaped curve.

Fig. 3 and Fig. 4 show the formation trajectories of USVs using control laws 1 and 2 respectively. Three USVs quickly assembled from the initial fragmented state into the linear shaped formation. At the time of 50 s ($x\approx 100$ m), the swarm reduces the speed and gathers the formation, and then it transforms into the triangle-shaped formation. At 100 s ($x\approx 150$ m), the swarm maintains the triangle-shaped formation and follows the S-shaped curve. It can be clearly seen that, compared with the control law 2, the USV assembles quickly during the whole voyage process with steady and smooth formation transformation under the guidance of control law 1. Furthermore, the swarm control effect is of great significance and strong flexibility.

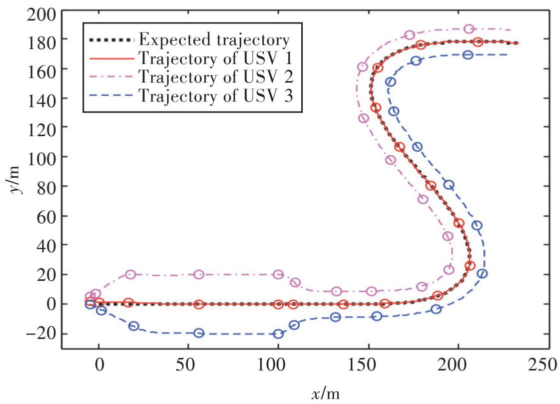

Fig.3 Formation trajectorys of USVs (control law 1)

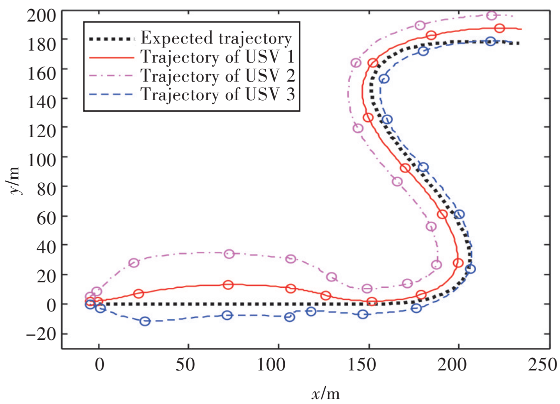

Fig.4 Formation trajectorys of USVs (control law 2)

Fig. 5 and Fig. 6 show the sailing speeds of three USVs under control laws 1 and 2, respectively. It can be seen that the surge velocity is finally maintained at about 1 m/s. Due to the existence of a curved trajectory, the sway velocity and the yawing angular velocity are not 0.

Fig. 7 and Fig. 8 show the control inputs of three

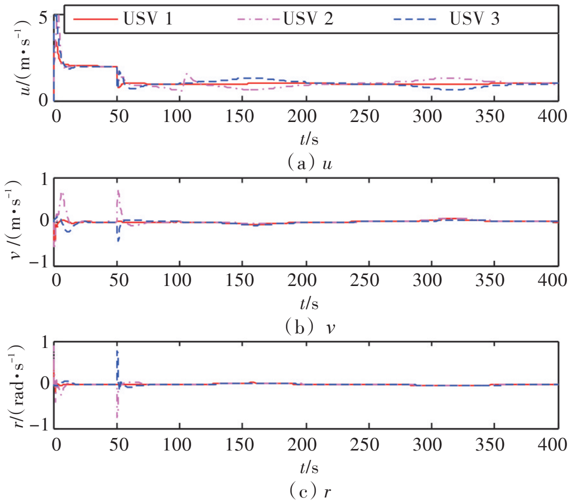

Fig.5 Velocities of USVs (control law 1)

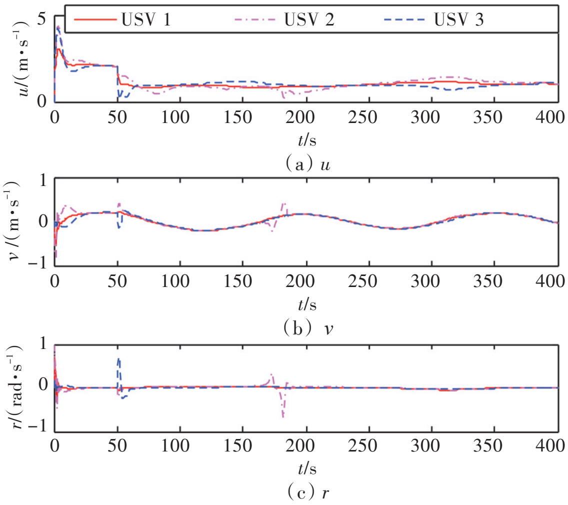

Fig.6 Velocities of USVs (control law 2)

USVs using control laws 1 and 2, respectively. It can be seen that the input curve is smooth and the buffeting is small, which can effectively reduce the mechanical loss of the thruster.

Fig. 9 and Fig. 10 show the tracking errors of three USVs using control laws 1 and 2, respectively. It can be seen that under the guidance of control law 1,

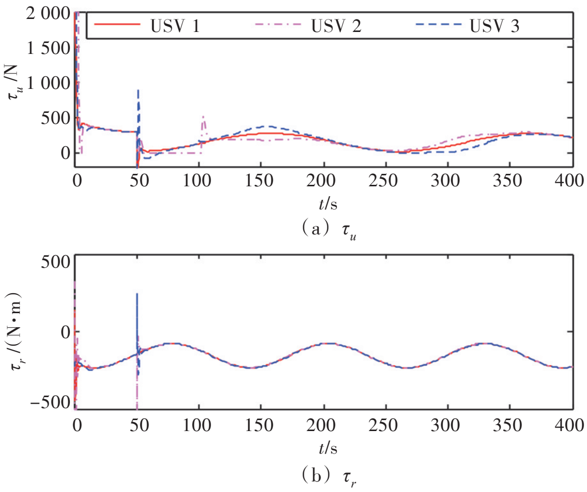

Fig.7 Control inputs of USVs (control law 1)

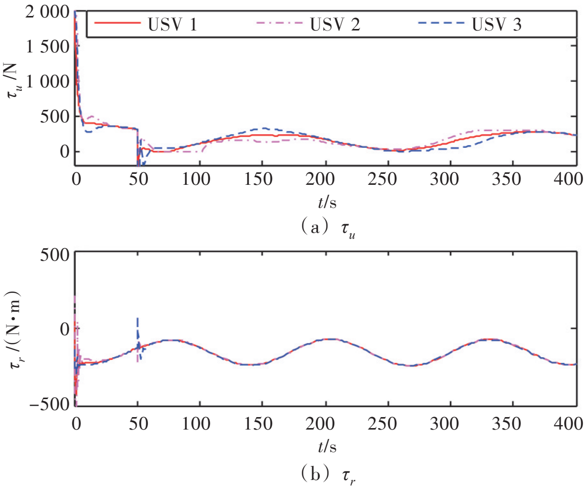

Fig.8 Control inputs of USVs (control law 2)

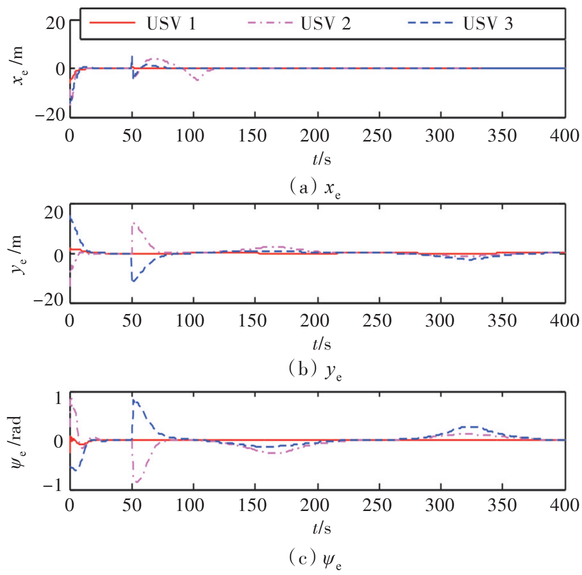

Fig.9 Tracking errors of USVs (control law 1)

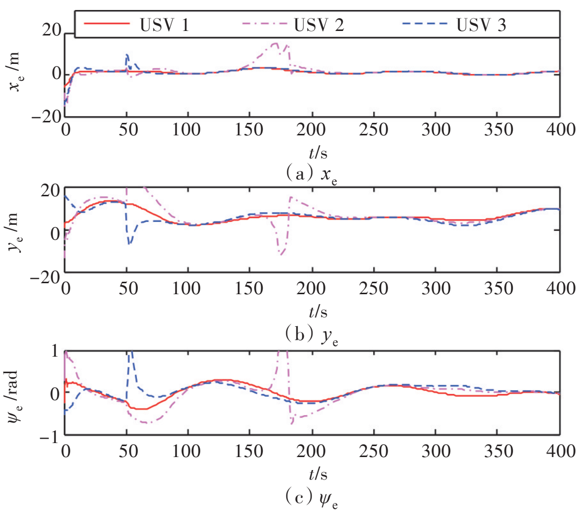

Fig.10 Tracking errors of USVs (control law 2)

the tracking errors of USVs converge uniformly and quickly to a small region near the origin point without overshoot. The control law in this paper has a good ability to compensate for uncertain external disturbances and has strong robustness. However, the navigation error of control law 2 is large and does not satisfy the accuracy requirement of control, which further verifies the feasibility and superiority of the control method in this paper.

5 Conclusions

Starting from the two aspects of kinematics and dynamics, and combining non-linear theories including backstepping method, sliding mode variable structure control, and Lyapunov stability, this paper adopts the swarm control strategy of the virtual structure method to study the control problem of underactuated USVs. Fully considering the system uncertainty and the influence of external environmental disturbance, the controller of the USVs based on adaptive backstepping with the sliding mode is designed, and the stability of the closed-loop system is proved. Simulation tests verify the feasibility and superiority of the control method in this paper. The specific performance is as follows: The USV swarm works well and the swarm formation transfers smoothly. Furthermore, the USV swarm can adaptively compensate for various uncertain disturbances and show strong robustness, flexibility, and adaptability. Furthermore, the predetermined control objectives are achieved, thus providing an effective basis for the practical application of USV control.

References

[1] Xu Y R, Su Y M, Pang Y J. Expectation of the development in the technology on ocean space intelligent unmanned vehicles [J]. Chinese Journal of Ship Research, 2006, 1(3): 1-4 (in Chinese).

[2] Cao S J, Zeng F M, Chen Y T. The course and speed cooperative control method for unmanned surface vehicles[J]. Chinese Journal of Ship Research, 2015, 10(6): 74-80 (in Chinese).

[3] Zhang B, Kang F J, Yan J T. Simulation of optimization model for attack mission planning of unmanned surface vessels cluster [J]. Computer Simulation, 2014, 31(11): 24-28 (in Chinese).

[4] Almeida J, Silvestre C, Pascoal A M. Cooperative control of multiple surface vessels with discrete-time periodic communications[J]. International Journal of Robust and Nonlinear Control, 2012, 22(4): 398-419.

[5] Campbell S, Naeem W, Irwin G W. A review on improving the autonomy of unmanned surface vehicles through intelligent collision avoidance manoeuvres[J]. Annual Reviews in Control, 2012, 36(2): 267-283.

[6] Shojaei K. Leader-follower formation control of underactuated autonomous marine surface vehicles with limited torque [J]. Ocean Engineering, 2015, 105: 196-205.

[7] Shen C, Shi Y, Buckham B. Trajectory tracking control of an autonomous underwater vehicle using Lyapunov-based model predictive control[J]. IEEE Transactions on Industrial Electronics, 2018, 65(7): 5796-5805.

[8] Shojaei K. Neural network formation control of underactuated autonomous underwater vehicles with saturating actuators[J]. Neurocomputing, 2016, 194: 372-384.

[9] Ding L, Guo G. Formation control for ship fleet based on backstepping[J]. Control and Decision, 2012, 27(2): 299-303 (in Chinese).

[10] Song Y R, Wang X P, Zhang S D, et al. Safeguarded formation control via the artificial potential method[J]. Journal of Naval Aeronautical Engineering Institute, 2011, 26(6): 622-627 (in Chinese).

[11] Monteiro S, Bicho E. A dynamical systems approach to behavior-based formation control[C]//Proceedings of 2002 IEEE International Conference on Robotics and Automation. Washington, DC, USA: IEEE, 2002.

[12] Zhao Y, Guo G, Ding L, et al. Collision/obstacle avoidance control of vessel formation[J]. Information and Control, 2012, 41(4): 425-432, 438 (in Chinese).

基于自适应反步滑模的水面无人艇集群控制

胡建章，唐国元*，王建军，解德

华中科技大学 船舶与海洋工程学院，湖北 武汉 430074

摘　要：［**目的**］针对多艘欠驱动水面无人艇组成的集群系统控制问题，研究虚拟结构法的控制策略。［**方法**］首先，将集群控制问题转化成无人艇与虚拟结构之间位姿跟踪误差的镇定问题，通过改变虚拟结构的几何形状，实现集群的队形变换。然后，将集群控制器的设计分为运动学和动力学2个部分，充分考虑不确定干扰，设计欠驱动水面无人艇集群的自适应反步滑模控制器，基于李雅普诺夫理论证明闭环系统的稳定性。最后，采取直、曲线航迹航行，开展集群队形变换等仿真试验。［**结果**］仿真结果表明，无人艇集群的协同运作效果显著，队形变换流畅，且能够自适应应对各种不确定干扰。［**结论**］集群系统展现出较强的鲁棒性与灵活性，可为后续实艇试验奠定理论基础。

关键词：集群控制；欠驱动无人艇；虚拟结构；自适应；反步法；滑模控制